CASCADED TRANSMISSION LINE MODEL FOR GLOBAL DTL ANALYSIS

J. Shmoys, R.M. Jones, and B.R. Cheo
Weber Research Institute, Polytechnic University, Farmingdale, NY 11735

Abstract

The structure of a DT linac is regarded as a tandem arrangement of sections of coaxial waveguide and circular waveguide. If these sections are long enough, the dominant mode is sufficient to represent propagation in each section. Thus the representation of the structure is reduced to a succession of transmission line segments connected by equivalent networks of the coaxial line-circular waveguide junctions. This equivalent network was calculated by the Galerkin procedure. This computation is the main CPU-time intensive ingredient of the theory and it is easily done on a PC. The complete calculation of field distribution and resonant frequency for a 30 drift tube linac takes about five minutes on a VAX. The tilt resulting from a perturbation of the end sections of the linac is easily calculated directly from the dimensions of the structure. For a uniform structure the agreement with results obtained by using the SUPERFISH program was excellent. One can incorporate into this model a representation of a post coupler as a series resonant circuit connected across the transmission line, with the two parameters determined by the length and thickness of the post. Numerical experiments show that the post coupler should be tuned below the cavity resonant frequency for stabilization.

Introduction

The DT Linac cavity consists of a long pipe in which a number of drift tubes are coaxially located as shown in Fig. 1. Neglecting for the moment the effect of the feed ports we see that the structure is a tandem arrangement of sections of circular and coaxial waveguides. The beam apertures are usually small enough compared to wavelength that their effect on field distribution can be neglected. If both the drift tube lengths and gaps are sufficiently long, the cavity can be represented by a series of cascaded transmission lines representing dominant mode propagation in the two waveguides joined through two-ports representing the junction of circular and coaxial waveguides (see Fig. 2).

The voltage-current transfer matrix of the junction is obtained from the scattering matrix, which in turn, is obtained by the Galerkin procedure.

The resonant frequency is calculated by recognizing that the voltage at the end of the cavity is zero, while the current can be set to an arbitrary value; this two-vector is then multiplied by each successive 2 x 2 transfer matrix until the opposite end of the cavity is reached; since the voltage at this end must also be zero, frequency is varied until this condition is satisfied. The dominant mode voltage distribution is then checked to identify the cavity mode.

Once the resonant frequency is found, the field distribution can be obtained. The dominant waveguide mode contributions are obtained directly from the voltages and currents previously calculated at each interface. In order to calculate higher order mode contributions, first the incident dominant mode wave amplitudes, from both sides, onto a junction are calculated from voltage and current; then, using the scattering coefficients obtained in the solution of the coaxial-circular waveguide discontinuity problem, the amplitudes of all higher order modes excited at each junction are calculated. Once the field distribution is known, stored energy in the cavity and wall losses can be calculated.

The Discontinuity Problem

The transverse part of the electromagnetic field in a homogeneously filled waveguide of uniform cross-section can be expressed in a modal series

$$\underline{E}_t(x,y,z) = \sum_n V_n(z)\,\underline{e}_n(x,y)\ , \tag{1}$$

$$\underline{H}_t(x,y,z) = \sum_n I_n(z)\,\underline{h}_n(x,y)\ , \tag{2}$$

when $\underline{e}_n$ and $\underline{h}_n$ are vector mode functions for electric and magnetic fields for the n^{th} mode, while V_n and I_n are voltage and current satisfying transmission line equations. In the case under consideration, only angularly independent TM modes are involved. In circular waveguide the mode functions are

$$\underline{e}_n = -\,\underline{r}_o \pi^{-1/2} J_1(\chi_n r/a)/aJ_1(\chi_n)\ ,\quad n = 1,2,\ldots\ , \tag{3}$$

where χ_n is the n^{th} root of $J_o(x) = 0$. Similarly, for the coaxial waveguide, the mode numbers $\hat{\chi}_m$ are the roots of $Z_o(\hat{\chi}_m a/b)$, where

$$Z_o(\hat{\chi}_m r/b) = \frac{\pi^{1/2}}{2}\,\frac{J_o(\hat{\chi}_m r/b)N_o(\hat{\chi}_m - N_o(\hat{\chi}_m r/b)J_o(\hat{\chi}_m)}{\left[J_o^2(\hat{\chi}_m)/J_o^2(a\hat{\chi}_m/b) - 1\right]^{1/2}} \tag{4}$$

and the mode functions are

$$\underline{\hat{e}}_m = -\,\underline{r}_o \hat{\chi}_m Z_o'(\hat{\chi}_m r/b)/b\ ,\quad m = 1,2,3,\ldots \tag{5a}$$

in addition to the TEM mode, for which

$$\underline{\hat{e}}_o = \underline{\hat{r}}(2\pi \ell n(a/b))^{-1/2}/r\ . \tag{5b}$$

The propagation constants of these modes are given by $\gamma_n = \sqrt{(\chi_n/a)^2 - (\omega/c)^2}$ and $\hat{\gamma}_m = \sqrt{(\hat{\chi}_m/b)^2 - (\omega/c)^2}$, where ω is the angular frequency and c is the velocity of light in free space. The wave impedance is given in both cases by $(\gamma/j\omega\epsilon_o)$. Due to the choice of normalization electric and magnetic mode functions are related by $\underline{h} = \underline{z}_o \times \underline{e}$.

The Galerkin procedure used here to solve the discontinuity problem makes use of the representation on both sides of the junction and of the continuity of tangential fields. For unit voltage incident wave, the transverse electric field is

$$\underline{E}_t = \underline{e}_1\, e^{-\gamma_1 z} + \sum_{n=1}^{\infty} \underline{e}_n S_{11,n} e^{\gamma_n z}\ , \tag{6}$$

where $S_{11,n}$ are as yet unknown scattering coefficients. The corresponding magnetic field is given by

$$-\,\underline{z}_o \times \underline{H}_t = \underline{e}_1 Y_1 e^{-\gamma_1 z} - \sum_{n=1}^{\infty} \underline{e}_n Y_n S_{11,n} e^{\gamma_n z}\ , \tag{7}$$

where Y_n is the modal wave admittance. Similarly, we have for the transmitted fields in the coaxial region

$$\underline{E}_t = \sum_{m=0}^{\infty} \underline{\hat{e}}_m S_{21,m} e^{\gamma_m z}\ , \tag{8}$$

$$-\,\underline{z}_o \times \underline{H}_t = \sum_{m=0}^{\infty} \underline{\hat{e}}_m\, \hat{Y}_m S_{21,m} e^{-\gamma_m z}\ . \tag{9}$$

We will eliminate $S_{11,n}$ and use $S_{21,m}$ as unknowns. Continuity of $\underline{E}_t$ at z= 0 yields, by equating Eq. (6) and Eq. (8), multiplying by $\underline{e}_\nu$ and integrating over the cross-section,

$$S_{11,\nu} + \delta^1_\nu = \sum_{m=0}^{\infty} P_{m\nu} S_{21,m} \,, \quad P_{m\nu} = \int \underline{e}_\nu \cdot \underline{\hat{e}}_m \, da, \quad (10)$$

the integral extending over the cross-section of the coaxial line. Equating $\underline{H}_t$ from Eq. (7) and Eq. (9) at z= 0, multiplying by $\underline{\hat{e}}_\mu$ and integrating gives

$$S_{21,\mu}\hat{Y}_\mu + \sum_{n=2}^{\infty} P_{n\mu} S_{11,n} Y_n + P_{1\mu}(S_{11,1} - 1) Y_1 = 0 \,. (11)$$

Substituting for $S_{11,n}$ from Eq. (10) and interchanging the order of summation, we obtain

$$S_{21,\mu}\hat{Y}_\mu + \sum_{m=0}^{\infty} S_{21,m} \left\{ \sum_{n=1}^{\infty} Y_n P_{mn} P_{n\mu} \right\} = 2 Y_1 P_{1\mu} \,. (12)$$

Since μ can take on any value, Eq. (12) is an infinite set of linear equations in an infinite number of unknowns $S_{21,m}$:

$$\sum_{m=0}^{\infty} A_{m\mu} S_{21,m} = B_\mu \,, \quad (13)$$

where $A_{m\mu} = \hat{Y}_\mu \delta^\mu_m + \sum_{n=i}^{\infty} Y_n P_{n\mu} P_{mn}$ and

$$B_\mu = 2 Y_1 P_{1\mu} \,.$$

This infinite set can be truncated so that the maximum value of m is of the order of 10 and the sum $A_{m\mu}$ usually converges rapidly enough so that 20 terms give sufficient accuracy. Once $S_{21,m}$ have been calculated $S_{11,n}$ can be obtained from Eq. (10).

For the case of incidence from the coaxial side we proceed in similar fashion, using the modified reflection coefficients $S_{22,m}+\delta^\circ_m$) as unknowns; we obtain for these a set of equations, with the same matrix $A_{m\mu}$, but with the inhomogeneous terms $B_\mu = 2\hat{Y}_\circ \delta^\mu_\circ$.
The transmission coefficients in this case are

$$S_{12,n} = \sum_{m=0}^{\infty} (S_{22,m}+\delta^\circ_m) P_{nm} \,. \quad (14)$$

The integration in the scalar products can be carried out explicitly and we obtain

$$P_{n0} = (2/\ell na/b)^{1/2} J_\circ(\chi_n b/a)/\chi_n J_1(\chi_n) \quad (15a)$$

$$P_{nm} = \frac{2\chi_n J_\circ(\chi_n b/a)/\left[\chi_n^2 - \hat{\chi}_m^2 a^2/b^2\right]}{J_1(\chi_n)\left[J^2_\circ(\hat{\chi}_m)/J^2_\circ(\hat{\chi}_m)/J^2_\circ(\hat{\chi}_m a/b) - 1\right]^{1/2}} \,,$$

$$m \neq 0 \,. \quad (15b)$$

Resonance Condition

The discontinuity problem discussed above yielded the unnormalized scattering matrix for the junction, where only the dominant modes are retained. For circuit calculations either a transfer-scattering matrix or a voltage-current transfer matrix is needed. The latter, denoted by T_{WC}, was chosen to simplify the computer program, its elements are simply related to the elements of the scattering matrix.

If the junction is reversed, with circular waveguide on the right, its voltage current transfer matrix T_{CW} is the inverse of T_{WC}. We will denote by T_n the transfer matrix of the n^{th} section of transmission line in the equivalent circuit. When n is odd, the transmission line is that for the dominant TM_{01} mode of the circular waveguide and when n is even, it is that for the TEM mode on the coaxial line. There are N coaxial sections (number of drift tubes) and N+ 1 circular waveguide sections.

The voltage at the right end of the structure is zero and the short-circuit current can be arbitrarily set to any convenient value $I_\circ$ since eventually all fields have to be multiplied by a constant which will insure proper normalization. The voltage and current at the left end terminals of the circuit shown in Fig. 1 are

$$\begin{pmatrix} V \\ I \end{pmatrix} = T_{2N+1} \cdot T_{WC} \cdot T_{CW} \cdots\cdots T_3 \cdot T_{WC} \cdot T_2 \cdot T_{CW} \cdot T_1 \cdot \begin{pmatrix} 0 \\ I_\circ \end{pmatrix}$$

Since all the transfer matrices are frequency-dependent, so is the terminal voltage V. Since, for cavity operation, this must be zero, we search for the resonant frequency $f_\circ$ such that $V(f_\circ) = 0$.

Numerical Results

The calculation of the scattering matrix of the discontinuity typically took into account 10 modes in the coaxial waveguide and about double that number in circular waveguide. This ratio, which depends on the ratio of waveguide to drift-tube diameters, must be maintained in order to avoid relative convergence problems normally associated with the Galerkin mode-matching procedure. Results obtained were in very good agreement with those obtained using the SUPERFISH program.

Field distributions obtained by the Galerkin method exhibit a behavior similar to the Gibbs' phenomenon (cf. Fig. 3). Hence no significance should be attached to values of fields calculated in the immediate vicinity of a junction. The more modes are taken into account, the narrower the region in which this occurs.

A sample field distribution for a ramp gradient linac is shown in Fig. 4.

Limitations of the Theory and Further Extensions

Clearly, if the drift-tube ends do not have the squared-off shape, the Galerkin procedure is not applicable, but the transfer matrix for the discontinuity can be evaluated by the application of the SUPERFISH program.

As was pointed out above, the transmission line representation of Fig. 2 is based on the assumption that higher order modes excited at one junction decay sufficiently by the time they reach the adjacent junction in either direction. In some cases the gap length is not consistent with this assumption, while the drift tube length might be sufficient. In that case the transfer matrix for the entire gap discontinuity, relative voltage, and current in the coaxial waveguide on one side of the gap to the voltage and current on the other side, should be used. If both gaps and drift tubes are too short, more than one transmission line may have to be used. In that case discontinuities have to be described by 4 x 4 or higher order matrices.

The presence of stems and posts destroys the rotational symmetry of the cavity. If coupling to asymmetrical modes could be assumed to be unimportant, than both of these structures could be represented by shunt elements.

This was done for posts, for which the circuit is a series resonant circuit. The resonant frequency depends primarily on the length of the post, while the L/C ratio depends on the post thickness.

Without tuning posts reducing the length of one end section of a drift tube and correspondingly increasing the length of the drift tube at the opposite end has little effect on the resonant frequency, but it produces a substantial ramp gradient. This gradient can be eliminated by tuning the shunt resonant circuits to a frequency about 1% below the original cavity resonance. More extensive studies of the sensitivity of the gap voltage distribution to end drift tube lengths were made using not the exact scattering matrix of the discontinuity but one for a series capacitance which differs from the exact matrix by about 10%. Gap voltage distributions for a 30 drift tube linac are shown on Fig. 5. These results are consistent with similar results obtained experimentally at LANL. The ratio of maximum to minimum gap voltage vs. post coupler resonant frequency is shown on Fig. 6.

Further work on improving and generalizing the cascaded transmission line model is continuing.

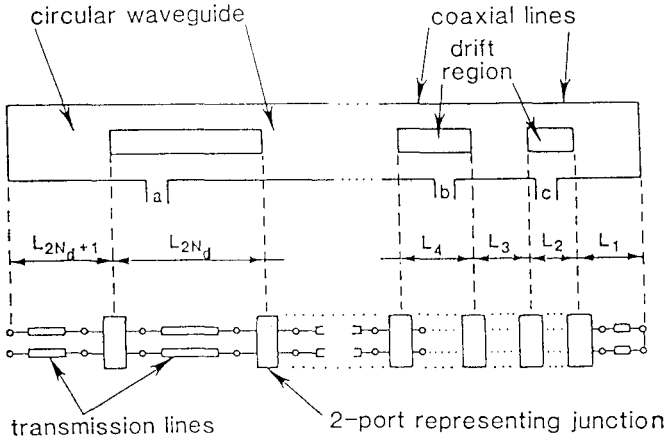

Fig. 1. Accelerator cavity and its transmission line mode.

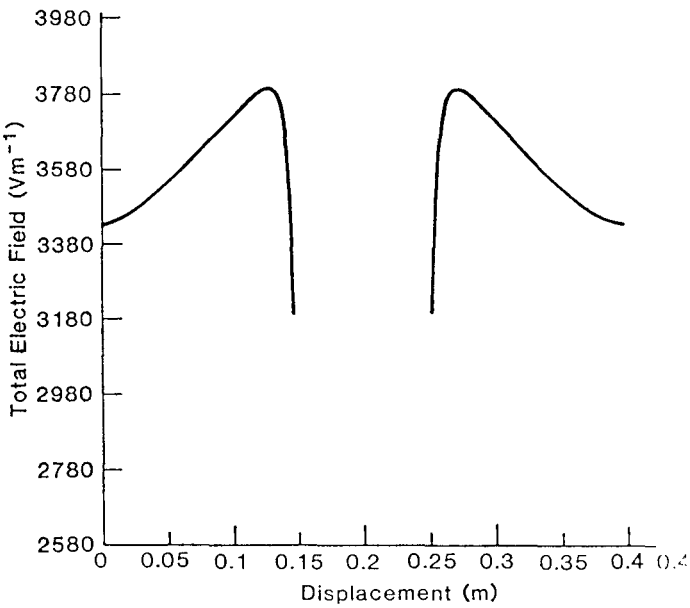

Fig 3. Axial electric field profile in gap regions from 0 to 0.15m and from 0.25 to 0.40m, for a single drift tube 0.1m long.

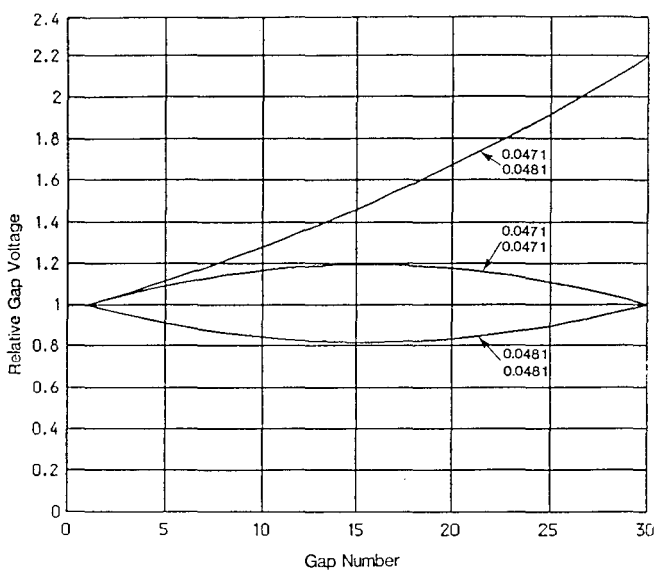

Fig. 5. Gap voltage distribution in a 30 section linac. All full length drift tubes 0.0952 m. long. End drift tubes as shown.

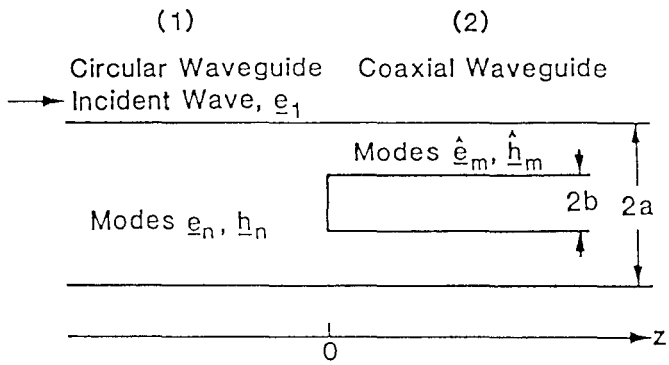

Fig. 2. Junction of circular and coaxial waveguides.

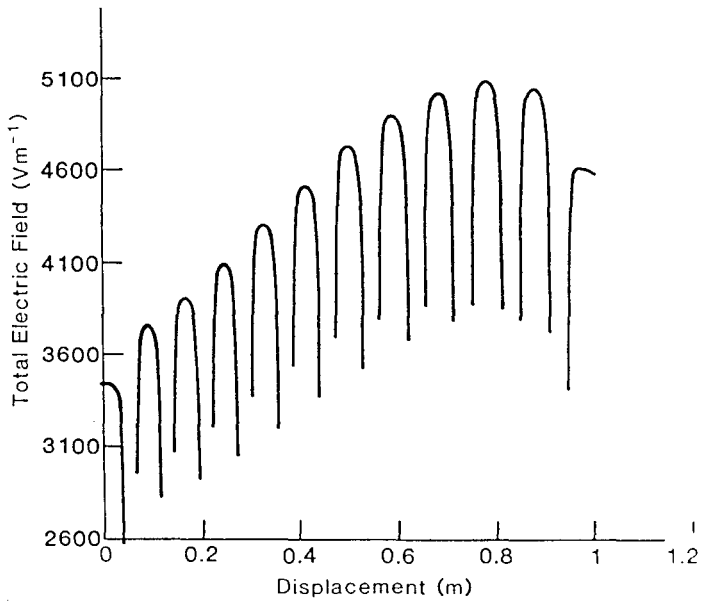

Fig. 4. Axial electric field as a function of the distance into the cavity (radius ration = 2, ramp gradient).

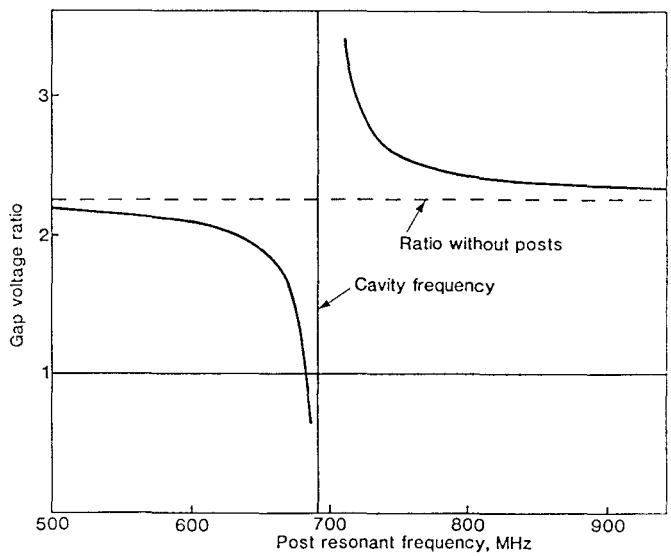

Fig. 6 Ratio of maximum to minimum gap voltage for linac as in Fig. 5, end drift tubes 0.0471m and 0.0481 m, vs. post coupler resonant frequency.

This work was supported by contract DNA00185C0182.